Supplementary Material

Toward the Searching for New Photosensitizers for DSSC: Theoretical Study of Both Substituted Zinc (II) and Si (IV) Phthalocyanines

Michael Zambrano-Angulo[a], and Gloria Cárdenas-Jirón*[a]

[a]*Laboratory of Theoretical Chemistry, Faculty of Chemistry and Biology, University of Santiago de Chile (USACH), Santiago, Chile*

*Corresponding author: gloria.cardenas@usach.cl

Table of Contents

S1. Molecular structure of phthalocyanines

Initially, to verify that the level of theory chosen is reliable for the systems to be evaluated, two similar systems reported experimentally were selected, which are a ZnPc without substituents and a SiPc with substituents in axial position. These systems were optimized to the B3LYP/6-31G(d,p) level of theory, adding the Grimme dispersion (D3). Comparing the values of the bond distances and bond angles of the experimentally reported systems with those obtained theoretically, a Root Mean Square Deviation (RMSD) value of 0.074 Å was obtained for the bond distances and 0.70° for the bond angles in the case of ZnPc. On the other hand, silicon-based phthalocyanines predict RMSD values of 0.019 Å and 2.18° for distances and bond angles, respectively. These results demonstrate that the choice of the level of theory for the description of the structure of the systems to be evaluated is optimal and generates reliable results.

Once the functional was chosen, we performed the complete geometry optimization of each phthalocyanine in the gas phase using the hybrid functional B3LYP with the basis set 6-31G(d,p) and Grimme dispersion correction (D3). A set of 33 substituted **ZnPc** species and 33 substituted **SiPc** species were investigated. For each metal, we optimize three sets of 11 compounds, each one that differs in the anchoring group (R_2, Scheme 1); anhydrous (**A**), carboxyl (**B**), and catechol (**C**), and with a singlet spin multiplicity and a neutral total charge.

ZnPc-Anhydrous (A)

ZnPc-1A	**ZnPc-2A**	**ZnPc-3A**	**ZnPc-4A**
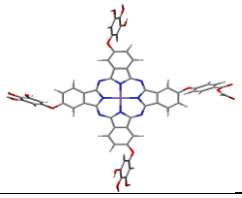	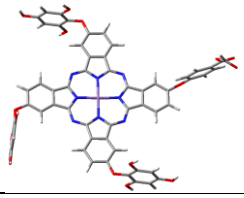	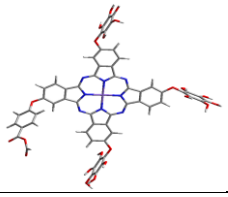	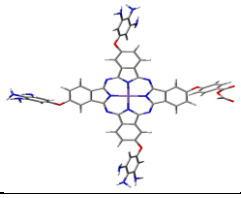

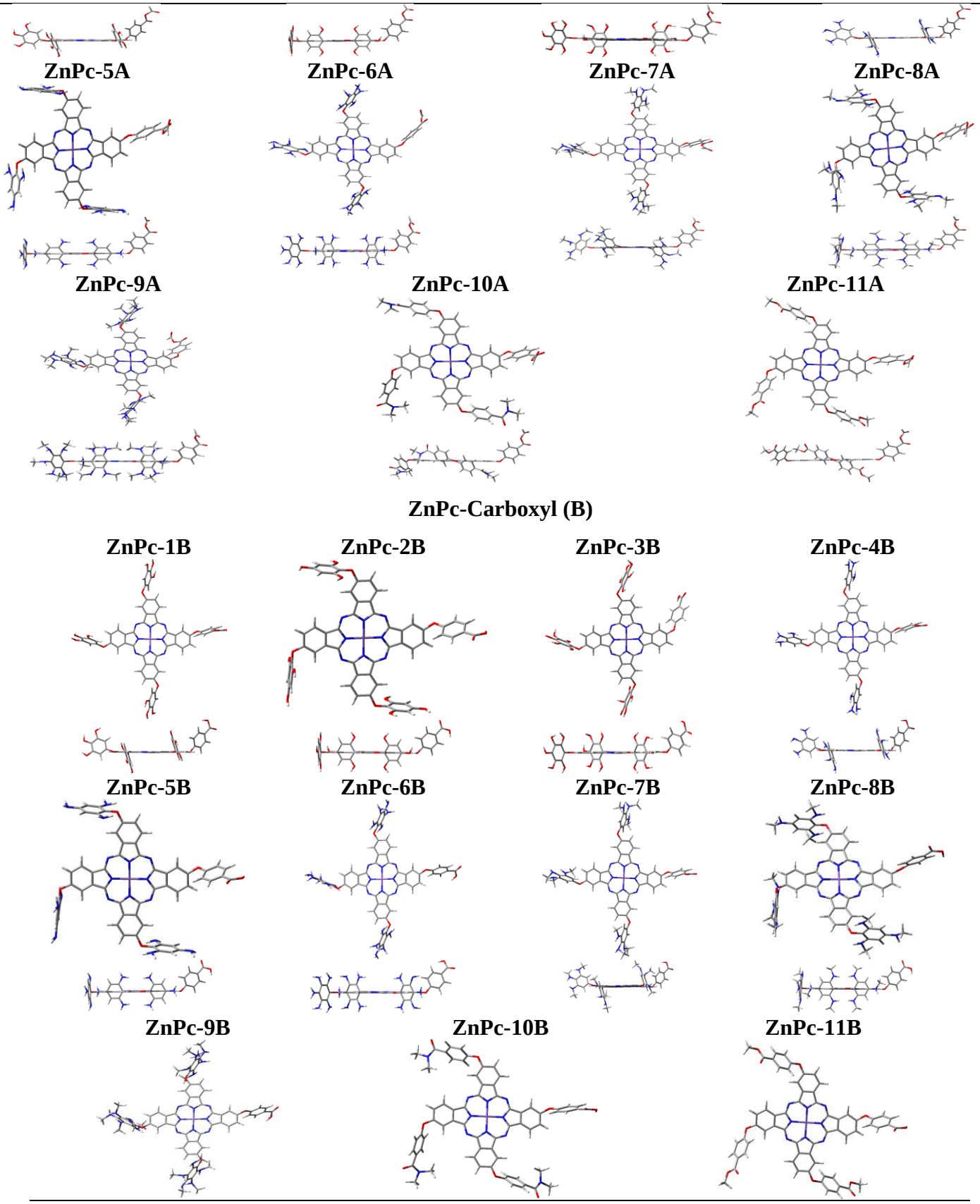
ZnPc-5A
ZnPc-6A
ZnPc-7A
ZnPc-8A
ZnPc-9A
ZnPc-10A
ZnPc-11A
ZnPc-Carboxyl (B)
ZnPc-1B
ZnPc-2B
ZnPc-3B
ZnPc-4B
ZnPc-5B
ZnPc-6B
ZnPc-7B
ZnPc-8B
ZnPc-9B
ZnPc-10B
ZnPc-11B

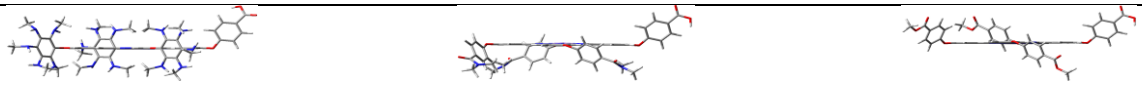

ZnPc-Catechol (C)

ZnPc-1C

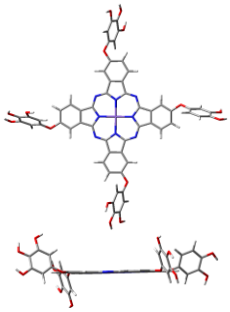

ZnPc-2C

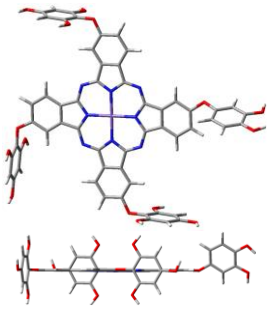

ZnPc-3C

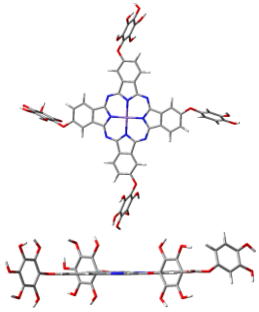

ZnPc-4C

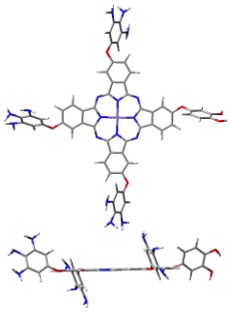

ZnPc-5C

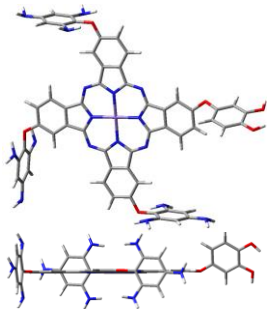

ZnPc-6C

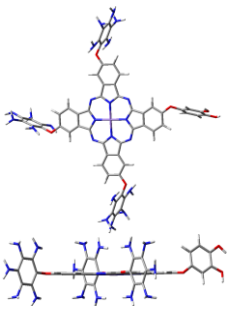

ZnPc-7C

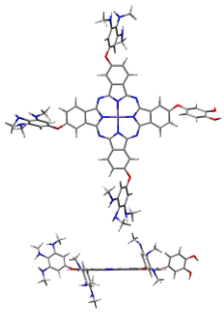

ZnPc-8C

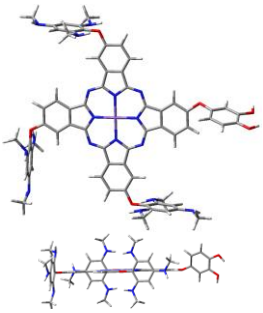

ZnPc-9C

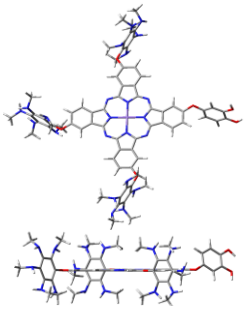

ZnPc-10C

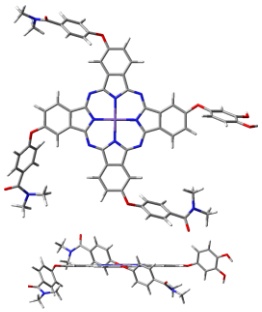

ZnPc-11C

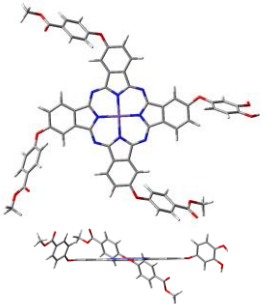

SiPc-Anhydrous (A)

SiPc-1A

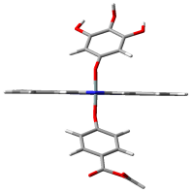

SiPc-2A

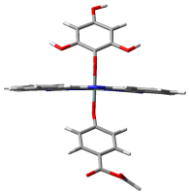

SiPc-3A

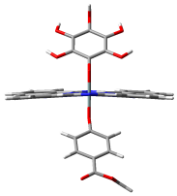

SiPc-4A

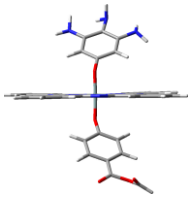

SiPc-5A

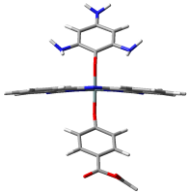

SiPc-6A

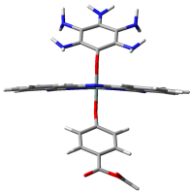

SiPc-7A **SiPc-8A** **SiPc-9A** **SiPc-10A** **SiPc-11A**

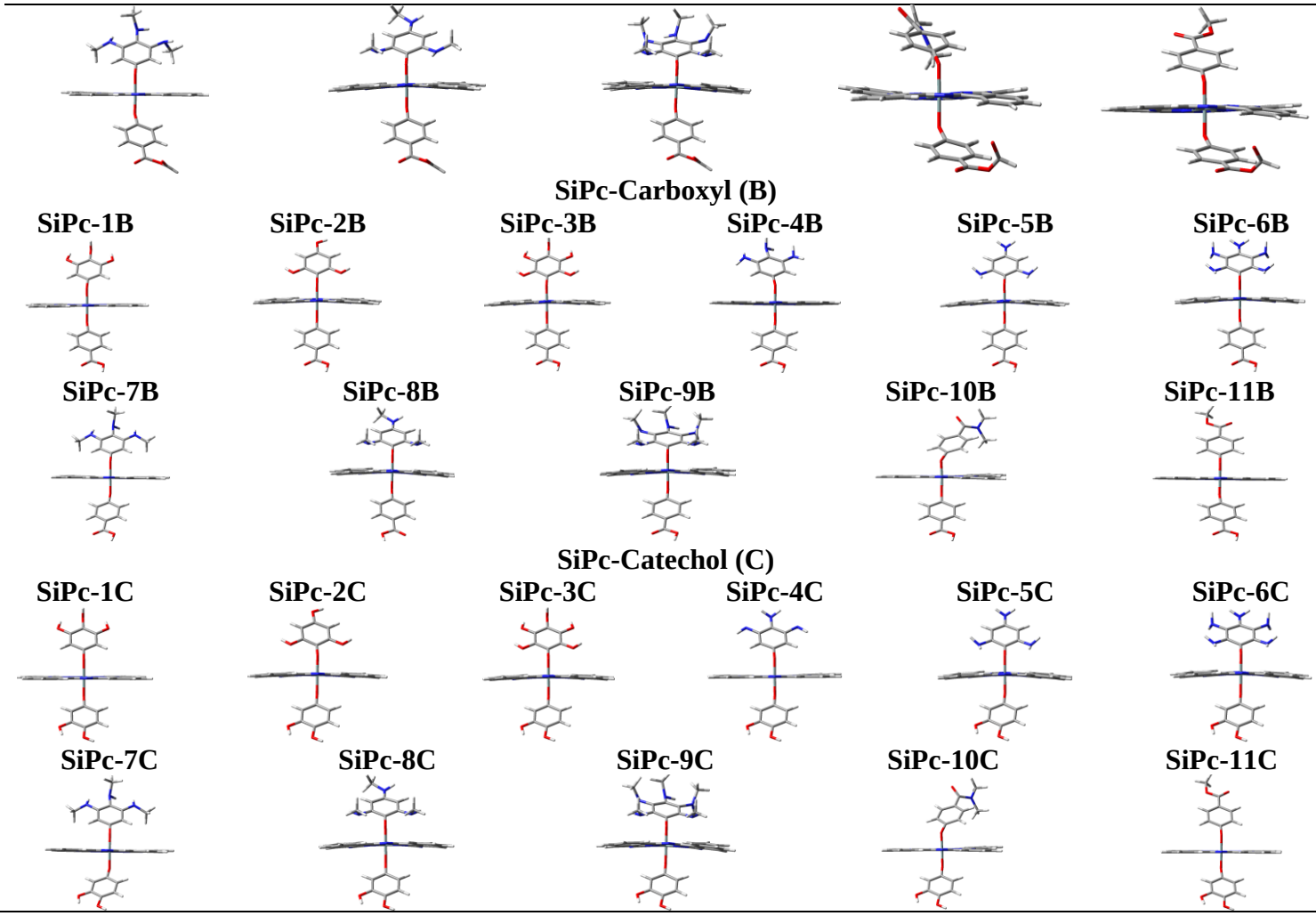

Figure SI. Molecular structures of **ZnPc** and **SiPc** with an anhydrous (**A**), carboxyl (**B**) and catechol (**C**) optimized at B3LYP/6-31G(d,p)/D3 level of theory.

The optimized species are presented in Figure SI. Those results were confirmed that are minimum energy states through the calculation of the vibrational frequencies where in all cases, positive values were obtained. For both metals, the phthalocyanine core is planar, and the substituents are located above and below the plane of the macrocycle, thus generating non-planar structures with less tendency to aggregation and, therefore, greater solubility. This effect is more significant in silicon phthalocyanines due to the axial position of the substituents, which allows for this metal to have a coordination of octahedral.

To simplify the analysis, we select the bonds N-metal, where N is the isoindoline nitrogen atom (Figure SII). The optimized bond distances (N-metal) for all the structures are compared with those reported experimentally for **ZnPc** without substituents and **SiPc** with substitution in the axial position by phenoxy groups. The theoretical values of the bond distances N-Zn and N-Si are compared with the experimental reported; 1.97 and 1.92 Å for the N-Zn and N-Si bonds, respectively. As for the systems without any type of substitution (ZnPc and $SiPcCl_2$), the bond distances between the central atom and the nitrogens of the macrocycle were similar to those obtained with the substitutions evaluated, where for silicon a bond distance of 1,92 Å was found, which was shorter than the 1,90 Å found for zinc.

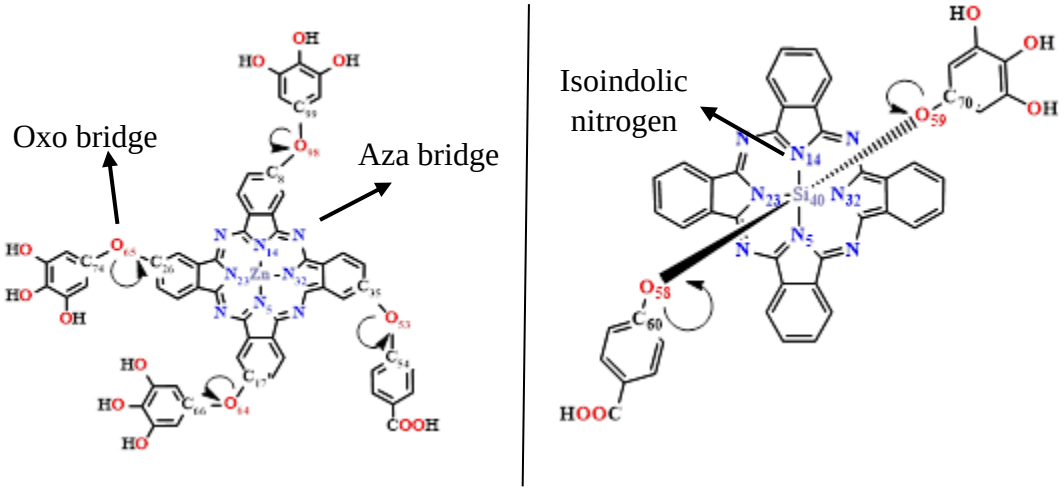

Figure SII. Atoms labels for the substituted MPcs. Left: ZnPc. Right: SiPc.

The angles that involve the substituent group and anchoring group are also shown. Table SI shows the results for substituted **ZnPc** and **SiPc** with three anchoring groups (R_2). As can be seen in Table SI, the results obtained for the distances between isoindoline nitrogen and the central atom for both systems are very close to the experimental data, obtaining an error of 1.01 % in the case of zinc phthalocyanines and a smaller value for their silicon

analogs (0.48 %). The results shown are for systems with anhydrous as the anchor group; however, for anchoring groups, carboxyl (**B**) and catechol (**C**) presented an error of 1.01 and 1.02 %, respectively, in the case of ZnPc and 0.61 (**B**) and 0.70 (**C**) for SiPc systems. Finally, these values demonstrate once again that the choice of the level of theory was suitable.

Table SI. Main structural parameters calculated for **1A** of both MPcs. Distances in angstroms (Å) and angles are reported in degrees (°).

ZnPc 1A				**SiPc 1A**			
Distance (Å)		Angles (°)		Distance (Å)		Angles (°)	
N_5-Zn_{41}	1.991	C_8-O_{98}-C_{99}	120.38	N_5-Si_{41}	1.930	Si_{41}-O_{59}-C_{70}	130.61
N_{23}-Zn_{41}	1.989	C_{26}-O_{65}-C_{74}	119.76	N_{23}-Si_{41}	1.937	Si_{41}-O_{58}-C_{60}	130.96
N_{14}-Zn_{41}	1.991	C_{17}-O_{64}-C_{66}	120.45	N_{14}-Si_{41}	1.934		
N_{32}-Zn_{41}	1.991	C_{35}-O_{53}-C_{54}	120.25	N_{32}-Si_{41}	1.930		
ZnPc 2A				**SiPc 2A**			
N_5-Zn_{41}	1.989	C_8-O_{86}-C_{87}	118.872	N_5-Si_{41}	1.930	Si_{41}-O_{59}-C_{70}	129.52
N_{23}-Zn_{41}	1.987	C_{26}-O_{65}-C_{72}	118.917	N_{23}-Si_{41}	1.931	Si_{41}-O_{58}-C_{60}	131.44
N_{14}-Zn_{41}	1.991	C_{17}-O_{64}-C_{66}	118.882	N_{14}-Si_{41}	1.934		
N_{32}-Zn_{41}	1.990	C_{35}-O_{53}-C_{54}	119.825	N_{32}-Si_{41}	1.930		
ZnPc 3A				**SiPc 3A**			
N_5-Zn_{41}	1.992	C_8-O_{86}-C_{87}	119.476	N_5-Si_{41}	1.929	Si_{41}-O_{59}-C_{70}	129.94
N_{23}-Zn_{41}	1.989	C_{26}-O_{65}-C_{72}	119.532	N_{23}-Si_{41}	1.929	Si_{41}-O_{58}-C_{60}	131.26
N_{14}-Zn_{41}	1.991	C_{17}-O_{64}-C_{66}	119.541	N_{14}-Si_{41}	1.932		
N_{32}-Zn_{41}	1.992	C_{35}-O_{53}-C_{54}	120.961	N_{32}-Si_{41}	1.929		
ZnPc 4A				**SiPc 4A**			
N_5-Zn_{41}	1.991	C_8-O_{86}-C_{87}	120.356	N_5-Si_{41}	1.931	Si_{41}-O_{59}-C_{70}	129.35
N_{23}-Zn_{41}	1.988	C_{26}-O_{65}-C_{72}	120.603	N_{23}-Si_{41}	1.938	Si_{41}-O_{58}-C_{60}	131.09
N_{14}-Zn_{41}	1.990	C_{17}-O_{64}-C_{66}	120.433	N_{14}-Si_{41}	1.935		
N_{32}-Zn_{41}	1.992	C_{35}-O_{53}-C_{54}	119.944	N_{32}-Si_{41}	1.931		
ZnPc 5A				**SiPc 5A**			
N_5-Zn_{41}	1.990	C_8-O_{86}-C_{87}	118.646	N_5-Si_{41}	1.932	Si_{41}-O_{59}-C_{70}	126.42
N_{23}-Zn_{41}	1.988	C_{26}-O_{65}-C_{72}	118.639	N_{23}-Si_{41}	1.932	Si_{41}-O_{58}-C_{60}	131.74
N_{14}-Zn_{41}	1.989	C_{17}-O_{64}-C_{66}	118.620	N_{14}-Si_{41}	1.930		
N_{32}-Zn_{41}	1.993	C_{35}-O_{53}-C_{54}	119.599	N_{32}-Si_{41}	1.925		
ZnPc 6A				**SiPc 6A**			
N_5-Zn_{41}	1.991	C_8-O_{86}-C_{87}	119.087	N_5-Si_{41}	1.932	Si_{41}-O_{59}-C_{70}	125.13
N_{23}-Zn_{41}	1.988	C_{26}-O_{65}-C_{72}	119.205	N_{23}-Si_{41}	1.931	Si_{41}-O_{58}-C_{60}	131.65
N_{14}-Zn_{41}	1.991	C_{17}-O_{64}-C_{66}	119.219	N_{14}-Si_{41}	1.931		
N_{32}-Zn_{41}	1.993	C_{35}-O_{53}-C_{54}	120.970	N_{32}-Si_{41}	1.927		
ZnPc 7A				**SiPc 7A**			
N_5-Zn_{41}	1.991	C_8-O_{86}-C_{87}	120.274	N_5-Si_{41}	1.933	Si_{41}-O_{59}-C_{70}	130.45
N_{23}-Zn_{41}	1.988	C_{26}-O_{65}-C_{72}	119.993	N_{23}-Si_{41}	1.937	Si_{41}-O_{58}-C_{60}	131.03
N_{14}-Zn_{41}	1.990	C_{17}-O_{64}-C_{66}	120.281	N_{14}-Si_{41}	1.935		
N_{32}-Zn_{41}	1.992	C_{35}-O_{53}-C_{54}	120.044	N_{32}-Si_{41}	1.931		

ZnPc 8A				**SiPc 8A**			
N_5-Zn_{41}	1.990	C_8-O_{86}-C_{87}	118.452	N_5-Si_{41}	1.930	Si_{41}-O_{59}-C_{70}	125.70
N_{23}-Zn_{41}	1.987	C_{26}-O_{65}-C_{72}	118.631	N_{23}-Si_{41}	1.935	Si_{41}-O_{58}-C_{60}	131.53
N_{14}-Zn_{41}	1.989	C_{17}-O_{64}-C_{66}	118.440	N_{14}-Si_{41}	1.932		
N_{32}-Zn_{41}	1.993	C_{35}-O_{53}-C_{54}	119.572	N_{32}-Si_{41}	1.923		
ZnPc 9A				**SiPc 9A**			
N_5-Zn_{41}	1.990	C_8-O_{86}-C_{87}	118.984	N_5-Si_{41}	1.930	Si_{41}-O_{59}-C_{70}	124.76
N_{23}-Zn_{41}	1.989	C_{26}-O_{65}-C_{72}	118.733	N_{23}-Si_{41}	1.927	Si_{41}-O_{58}-C_{60}	131.54
N_{14}-Zn_{41}	1.990	C_{17}-O_{64}-C_{66}	118.854	N_{14}-Si_{41}	1.929		
N_{32}-Zn_{41}	1.992	C_{35}-O_{53}-C_{54}	120.910	N_{32}-Si_{41}	1.926		
ZnPc 10A				**SiPc 10A**			
N_5-Zn_{41}	1.990	C_8-O_{86}-C_{87}	121.063	N_5-Si_{41}	1.922	Si_{41}-O_{59}-C_{70}	123.51
N_{23}-Zn_{41}	1.989	C_{26}-O_{65}-C_{72}	120.854	N_{23}-Si_{41}	1.920	Si_{41}-O_{58}-C_{60}	124.00
N_{14}-Zn_{41}	1.990	C_{17}-O_{64}-C_{66}	120.944	N_{14}-Si_{41}	1.926		
N_{32}-Zn_{41}	1.991	C_{35}-O_{53}-C_{54}	120.422	N_{32}-Si_{41}	1.920		
ZnPc 11A				**SiPc 11A**			
N_5-Zn_{41}	1.990	C_8-O_{86}-C_{87}	121.461	N_5-Si_{41}	1.922	Si_{41}-O_{59}-C_{70}	125.90
N_{23}-Zn_{41}	1.989	C_{26}-O_{65}-C_{72}	121.227	N_{23}-Si_{41}	1.924	Si_{41}-O_{58}-C_{60}	124.05
N_{14}-Zn_{41}	1.990	C_{17}-O_{64}-C_{66}	121.402	N_{14}-Si_{41}	1.924		
N_{32}-Zn_{41}	1.991	C_{35}-O_{53}-C_{54}	120.600	N_{32}-Si_{41}	1.916		
ZnPc 1B				**SiPc 1B**			
N_5-Zn_{41}	1.991	C_8-O_{86}-C_{87}	120.452	N_5-Si_{41}	1.932	Si_{41}-O_{59}-C_{70}	130.81
N_{23}-Zn_{41}	1.989	C_{26}-O_{65}-C_{72}	119.829	N_{23}-Si_{41}	1.936	Si_{41}-O_{58}-C_{60}	131.08
N_{14}-Zn_{41}	1.991	C_{17}-O_{64}-C_{66}	120.505	N_{14}-Si_{41}	1.933		
N_{32}-Zn_{41}	1.991	C_{35}-O_{53}-C_{54}	120.029	N_{32}-Si_{41}	1.931		
ZnPc 2B				**SiPc 2B**			
N_5-Zn_{41}	1.989	C_8-O_{86}-C_{87}	118.834	N_5-Si_{41}	1.930	Si_{41}-O_{59}-C_{70}	129.47
N_{23}-Zn_{41}	1.987	C_{26}-O_{65}-C_{72}	118.824	N_{23}-Si_{41}	1.931	Si_{41}-O_{58}-C_{60}	131.33
N_{14}-Zn_{41}	1.989	C_{17}-O_{64}-C_{66}	118.829	N_{14}-Si_{41}	1.933		
N_{32}-Zn_{41}	1.992	C_{35}-O_{53}-C_{54}	120.161	N_{32}-Si_{41}	1.932		
ZnPc 3B				**SiPc 3B**			
N_5-Zn_{41}	1.992	C_8-O_{86}-C_{87}	119.120	N_5-Si_{41}	1.929	Si_{41}-O_{59}-C_{70}	129.96
N_{23}-Zn_{41}	1.989	C_{26}-O_{65}-C_{72}	119.133	N_{23}-Si_{41}	1.930	Si_{41}-O_{58}-C_{60}	131.36
N_{14}-Zn_{41}	1.991	C_{17}-O_{64}-C_{66}	119.151	N_{14}-Si_{41}	1.932		
N_{32}-Zn_{41}	1.992	C_{35}-O_{53}-C_{54}	120.680	N_{32}-Si_{41}	1.930		
ZnPc 4B				**SiPc 4B**			
N_5-Zn_{41}	1.991	C_8-O_{86}-C_{87}	120.393	N_5-Si_{41}	1.937	Si_{41}-O_{59}-C_{70}	129.44
N_{23}-Zn_{41}	1.988	C_{26}-O_{65}-C_{72}	120.653	N_{23}-Si_{41}	1.933	Si_{41}-O_{58}-C_{60}	131.19
N_{14}-Zn_{41}	1.991	C_{17}-O_{64}-C_{66}	120.471	N_{14}-Si_{41}	1.933		
N_{32}-Zn_{41}	1.992	C_{35}-O_{53}-C_{54}	119.877	N_{32}-Si_{41}	1.934		
ZnPc 5B				**SiPc 5B**			
N_5-Zn_{41}	1.990	C_8-O_{86}-C_{87}	118.572	N_5-Si_{41}	1.932	Si_{41}-O_{59}-C_{70}	126.36
N_{23}-Zn_{41}	1.988	C_{26}-O_{65}-C_{72}	118.625	N_{23}-Si_{41}	1.932	Si_{41}-O_{58}-C_{60}	131.71
N_{14}-Zn_{41}	1.989	C_{17}-O_{64}-C_{66}	118.532	N_{14}-Si_{41}	1.929		
N_{32}-Zn_{41}	1.992	C_{35}-O_{53}-C_{54}	120.117	N_{32}-Si_{41}	1.928		
ZnPc 6B				**SiPc 6B**			
N_5-Zn_{41}	1.990	C_8-O_{86}-C_{87}	119.099	N_5-Si_{41}	1.932	Si_{41}-O_{59}-C_{70}	125.02
N_{23}-Zn_{41}	1.988	C_{26}-O_{65}-C_{72}	119.092	N_{23}-Si_{41}	1.931	Si_{41}-O_{58}-C_{60}	131.74
N_{14}-Zn_{41}	1.991	C_{17}-O_{64}-C_{66}	119.157	N_{14}-Si_{41}	1.932		

N_{32}-Zn_{41}	1.992	C_{35}-O_{53}-C_{54}	119.947	N_{32}-Si_{41}	1.929		
ZnPc 7B				**SiPc 7B**			
N_5-Zn_{41}	1.990	C_8-O_{86}-C_{87}	119.964	N_5-Si_{41}	1.934	Si_{41}-O_{59}-C_{70}	130.42
N_{23}-Zn_{41}	1.988	C_{26}-O_{65}-C_{72}	120.057	N_{23}-Si_{41}	1.937	Si_{41}-O_{58}-C_{60}	131.27
N_{14}-Zn_{41}	1.990	C_{17}-O_{64}-C_{66}	120.037	N_{14}-Si_{41}	1.933		
N_{32}-Zn_{41}	1.992	C_{35}-O_{53}-C_{54}	119.680	N_{32}-Si_{41}	1.935		
ZnPc 8B				**SiPc 8B**			
N_5-Zn_{41}	1.989	C_8-O_{86}-C_{87}	118.002	N_5-Si_{41}	1.932	Si_{41}-O_{59}-C_{70}	126.30
N_{23}-Zn_{41}	1.987	C_{26}-O_{65}-C_{72}	117.964	N_{23}-Si_{41}	1.931	Si_{41}-O_{58}-C_{60}	131.73
N_{14}-Zn_{41}	1.989	C_{17}-O_{64}-C_{66}	117.986	N_{14}-Si_{41}	1.929		
N_{32}-Zn_{41}	1.992	C_{35}-O_{53}-C_{54}	119.681	N_{32}-Si_{41}	1.927		
ZnPc 9B				**SiPc 9B**			
N_5-Zn_{41}	1.990	C_8-O_{86}-C_{87}	119.098	N_5-Si_{41}	1.928	Si_{41}-O_{59}-C_{70}	125.17
N_{23}-Zn_{41}	1.989	C_{26}-O_{65}-C_{72}	118.811	N_{23}-Si_{41}	1.930	Si_{41}-O_{58}-C_{60}	131.77
N_{14}-Zn_{41}	1.991	C_{17}-O_{64}-C_{66}	118.792	N_{14}-Si_{41}	1.927		
N_{32}-Zn_{41}	1.992	C_{35}-O_{53}-C_{54}	119.376	N_{32}-Si_{41}	1.929		
ZnPc 10B				**SiPc 10B**			
N_5-Zn_{41}	1.990	C_8-O_{86}-C_{87}	120.384	N_5-Si_{41}	1.925	Si_{41}-O_{59}-C_{70}	128.53
N_{23}-Zn_{41}	1.990	C_{26}-O_{65}-C_{72}	120.206	N_{23}-Si_{41}	1.939	Si_{41}-O_{58}-C_{60}	130.94
N_{14}-Zn_{41}	1.991	C_{17}-O_{64}-C_{66}	120.621	N_{14}-Si_{41}	1.935		
N_{32}-Zn_{41}	1.992	C_{35}-O_{53}-C_{54}	120.177	N_{32}-Si_{41}	1.935		
ZnPc 11B				**SiPc 11B**			
N_5-Zn_{41}	1.990	C_8-O_{86}-C_{87}	121.041	N_5-Si_{41}	1.933	Si_{41}-O_{59}-C_{70}	130.96
N_{23}-Zn_{41}	1.989	C_{26}-O_{65}-C_{72}	121.227	N_{23}-Si_{41}	1.932	Si_{41}-O_{58}-C_{60}	130.98
N_{14}-Zn_{41}	1.990	C_{17}-O_{64}-C_{66}	121.041	N_{14}-Si_{41}	1.934		
N_{32}-Zn_{41}	1.990	C_{35}-O_{53}-C_{54}	120.244	N_{32}-Si_{41}	1.931		
ZnPc 1C				**SiPc 1C**			
N_5-Zn_{41}	1.991	C_8-O_{86}-C_{87}	120.398	N_5-Si_{41}	1.934	Si_{41}-O_{59}-C_{69}	131.10
N_{23}-Zn_{41}	1.991	C_{26}-O_{65}-C_{72}	119.991	N_{23}-Si_{41}	1.936	Si_{41}-O_{58}-C_{60}	130.42
N_{14}-Zn_{41}	1.991	C_{17}-O_{64}-C_{66}	120.364	N_{14}-Si_{41}	1.934		
N_{32}-Zn_{41}	1.990	C_{35}-O_{53}-C_{54}	120.231	N_{32}-Si_{41}	1.935		
ZnPc 2C				**SiPc 2C**			
N_5-Zn_{41}	1.990	C_8-O_{86}-C_{87}	120.384	N_5-Si_{41}	1.932	Si_{41}-O_{59}-C_{69}	129.76
N_{23}-Zn_{41}	1.990	C_{26}-O_{65}-C_{72}	120.206	N_{23}-Si_{41}	1.932	Si_{41}-O_{58}-C_{60}	130.61
N_{14}-Zn_{41}	1.991	C_{17}-O_{64}-C_{66}	120.621	N_{14}-Si_{41}	1.934		
N_{32}-Zn_{41}	1.992	C_{35}-O_{53}-C_{54}	120.177	N_{32}-Si_{41}	1.936		
ZnPc 3C				**SiPc 3C**			
N_5-Zn_{41}	1.990	C_8-O_{86}-C_{87}	120.384	N_5-Si_{41}	1.930	Si_{41}-O_{59}-C_{69}	130.14
N_{23}-Zn_{41}	1.990	C_{26}-O_{65}-C_{72}	120.206	N_{23}-Si_{41}	1.931	Si_{41}-O_{58}-C_{60}	130.67
N_{14}-Zn_{41}	1.991	C_{17}-O_{64}-C_{66}	120.621	N_{14}-Si_{41}	1.932		
N_{32}-Zn_{41}	1.992	C_{35}-O_{53}-C_{54}	120.177	N_{32}-Si_{41}	1.934		
ZnPc 4C				**SiPc 4C**			
N_5-Zn_{41}	1.990	C_8-O_{86}-C_{87}	120.384	N_5-Si_{41}	1.937	Si_{41}-O_{59}-C_{69}	129.51
N_{23}-Zn_{41}	1.990	C_{26}-O_{65}-C_{72}	120.206	N_{23}-Si_{41}	1.936	Si_{41}-O_{58}-C_{60}	130.54
N_{14}-Zn_{41}	1.991	C_{17}-O_{64}-C_{66}	120.621	N_{14}-Si_{41}	1.936		
N_{32}-Zn_{41}	1.992	C_{35}-O_{53}-C_{54}	120.177	N_{32}-Si_{41}	1.937		
ZnPc 5C				**SiPc 5C**			
N_5-Zn_{41}	1.990	C_8-O_{86}-C_{87}	120.384	N_5-Si_{41}	1.933	Si_{41}-O_{59}-C_{69}	126.76
N_{23}-Zn_{41}	1.990	C_{26}-O_{65}-C_{72}	120.206	N_{23}-Si_{41}	1.934	Si_{41}-O_{58}-C_{60}	130.95

N_{14}-Zn_{41}	1.991	C_{17}-O_{64}-C_{66}	120.621	N_{14}-Si_{41}	1.929		
N_{32}-Zn_{41}	1.992	C_{35}-O_{53}-C_{54}	120.177	N_{32}-Si_{41}	1.932		
ZnPc 6C				**SiPc 6C**			
N_{5}-Zn_{41}	1.990	C_{8}-O_{86}-C_{87}	120.384	N_{5}-Si_{41}	1.932	Si_{41}-O_{59}-C_{69}	125.28
N_{23}-Zn_{41}	1.990	C_{26}-O_{65}-C_{72}	120.206	N_{23}-Si_{41}	1.934	Si_{41}-O_{58}-C_{60}	131.05
N_{14}-Zn_{41}	1.991	C_{17}-O_{64}-C_{66}	120.621	N_{14}-Si_{41}	1.931		
N_{32}-Zn_{41}	1.992	C_{35}-O_{53}-C_{54}	120.177	N_{32}-Si_{41}	1.933		
ZnPc 7C				**SiPc 7C**			
N_{5}-Zn_{41}	1.990	C_{8}-O_{86}-C_{87}	120.384	N_{5}-Si_{41}	1.932	Si_{41}-O_{59}-C_{69}	125.28
N_{23}-Zn_{41}	1.990	C_{26}-O_{65}-C_{72}	120.206	N_{23}-Si_{41}	1.934	Si_{41}-O_{58}-C_{60}	131.05
N_{14}-Zn_{41}	1.991	C_{17}-O_{64}-C_{66}	120.621	N_{14}-Si_{41}	1.931		
N_{32}-Zn_{41}	1.992	C_{35}-O_{53}-C_{54}	120.177	N_{32}-Si_{41}	1.933		
ZnPc 8C				**SiPc 8C**			
N_{5}-Zn_{41}	1.990	C_{8}-O_{86}-C_{87}	120.384	N_{5}-Si_{41}	1.931	Si_{41}-O_{59}-C_{69}	126.45
N_{23}-Zn_{41}	1.990	C_{26}-O_{65}-C_{72}	120.206	N_{23}-Si_{41}	1.933	Si_{41}-O_{58}-C_{60}	130.97
N_{14}-Zn_{41}	1.991	C_{17}-O_{64}-C_{66}	120.621	N_{14}-Si_{41}	1.930		
N_{32}-Zn_{41}	1.992	C_{35}-O_{53}-C_{54}	120.177	N_{32}-Si_{41}	1.930		
ZnPc 9C				**SiPc 9C**			
N_{5}-Zn_{41}	1.990	C_{8}-O_{86}-C_{87}	120.384	N_{5}-Si_{41}	1.928	Si_{41}-O_{59}-C_{69}	125.25
N_{23}-Zn_{41}	1.990	C_{26}-O_{65}-C_{72}	120.206	N_{23}-Si_{41}	1.932	Si_{41}-O_{58}-C_{60}	131.01
N_{14}-Zn_{41}	1.991	C_{17}-O_{64}-C_{66}	120.621	N_{14}-Si_{41}	1.928		
N_{32}-Zn_{41}	1.992	C_{35}-O_{53}-C_{54}	120.177	N_{32}-Si_{41}	1.931		
ZnPc 10C				**SiPc 10C**			
N_{5}-Zn_{41}	1.990	C_{8}-O_{86}-C_{87}	120.384	N_{5}-Si_{41}	1.926	Si_{41}-O_{59}-C_{69}	128.79
N_{23}-Zn_{41}	1.990	C_{26}-O_{65}-C_{72}	120.206	N_{23}-Si_{41}	1.940	Si_{41}-O_{58}-C_{60}	130.36
N_{14}-Zn_{41}	1.991	C_{17}-O_{64}-C_{66}	120.621	N_{14}-Si_{41}	1.935		
N_{32}-Zn_{41}	1.992	C_{35}-O_{53}-C_{54}	120.177	N_{32}-Si_{41}	1.939		
ZnPc 11C				**SiPc 11C**			
N_{5}-Zn_{41}	1.990	C_{8}-O_{86}-C_{87}	120.384	N_{5}-Si_{41}	1.935	Si_{41}-O_{59}-C_{69}	131.12
N_{23}-Zn_{41}	1.990	C_{26}-O_{65}-C_{72}	120.206	N_{23}-Si_{41}	1.932	Si_{41}-O_{58}-C_{60}	130.28
N_{14}-Zn_{41}	1.991	C_{17}-O_{64}-C_{66}	120.621	N_{14}-Si_{41}	1.937		
N_{32}-Zn_{41}	1.992	C_{35}-O_{53}-C_{54}	120.177	N_{32}-Si_{41}	1.932		

S2. Electronic properties of metal phthalocyanines

Once the molecular structures were optimized, the electronic properties were calculated (B3LYP/6-31G(d,p) level of theory) in the solution phase using the CPCM solvent model and the solvent tetrahydrofuran as it has been used in the experimental reports. For a better understanding of the following results, Figure SIII shows the labels of the atoms of interest. The atomic charges are obtained from the natural population analysis (NPA), and Table SII shows the results all systems for both phthalocyanines. The results show that for

both metals, the carbon atoms bonded to both indole and aza nitrogen atoms (Figure SIII) have a positive charge while the remaining carbon atoms have a negative charge. Additionally, in both systems, the deficiency in charge also is extended to the carbon atoms bonded to the oxo bridges of the substituents, as well as on the carbons directly attached to the hydroxyls and oxygen of the anchor group.

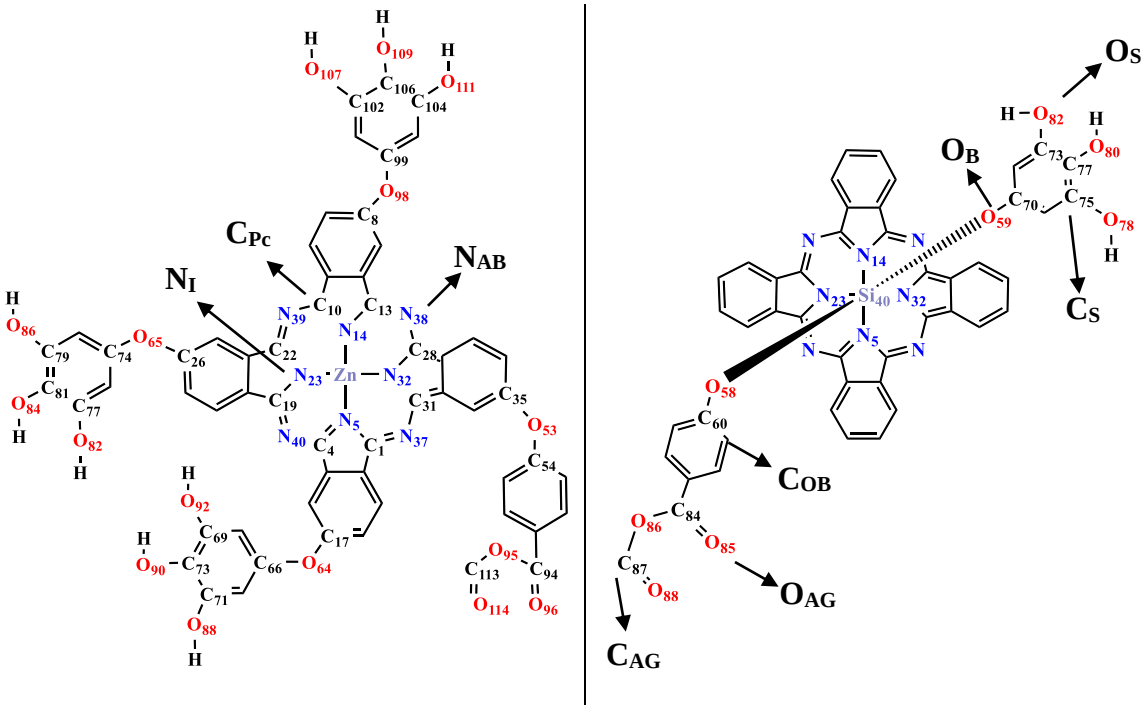

Figure SIII. Atoms labels for the MPcs. C_{AG}: Anchor group carbon, C_{Pc}: Phthalocyanine carbon, C_{OB}: Oxygen bridge carbon, C_S: Substituent carbon, N_{AB}: Aza bridge nitrogen, O_{OB}: Oxygen bridge, O_{AG}: Anchor group oxygen, N_I: Isoindolic nitrogen and O_S: Substituent oxygen.

The values reported in Table SII show an intramolecular charge transfer that goes from carbon atoms to nitrogen atoms (indole, aza) and to the oxygen atoms in the systems. In the same way, all nitrogen atoms in both systems have a negative charge, with the indole nitrogen atoms having the highest negative charge, this trend was also found for the systems without substituents. In the case of **ZnPc**, the indole nitrogen atoms have a charge of -0.68, while those aza bridges have a value of -0.50. This shows that the metal directly affects the

macrocycle through charge donation. This effect is slightly greater in **SiPc** for indole nitrogen (-0.71) compared to their zinc homologous (-0.68). The values in Table 2 are for systems with both central atoms and an anhydrous anchor group (**1A**). However, the analysis was performed for all studied systems in which the same trend was found.

Table SII. Main NPA charges from substituents and macrocycle obtained by NBO calculations at the B3LYP/6-31G(d,p)/D3 level of theory.

ZnPc -1A						SiPc-1A					
Atom		**Q**	**Atom**		**Q**	**Atom**		**Q**	**Atom**		**Q**
C_{AG}	94	0.824	C_S	73	0.197	C_{AG}	84	0.822	N_{AB}	38	-0.480
C_{AG}	113	0.663	N_{AB}	38	-0.496	C_{AG}	87	0.662	N_{AB}	37	-0.482
C_{Pc}	19	0.445	N_{AB}	37	-0.498	C_{Pc}	13	0.457	N_{AB}	39	-0.487
C_{Pc}	1	0.439	N_{AB}	39	-0.501	C_{Pc}	28	0.455	O_{AG}	85	-0.567
C_{Pc}	22	0.442	N_{AB}	40	-0.502	C_{Pc}	10	0.455	O_{AG}	88	-0.573
C_{Pc}	4	0.441	O_{OB}	53	-0.505	C_{Pc}	1	0.452	O_{AG}	86	-0.590
C_{Pc}	10	0.441	O_{OB}	64	-0.514	C_{Pc}	19	0.454	N_I	32	-0.703
C_{Pc}	13	0.435	O_{OB}	98	-0.514	C_{Pc}	31	0.454	O_S	78	-0.705
C_{Pc}	28	0.431	O_{OB}	65	-0.515	C_{Pc}	4	0.452	O_S	82	-0.705
C_{Pc}	31	0.430	O_{AG}	96	-0.565	C_{Pc}	22	0.451	N_I	5	-0.705
C_{OB}	54	0.347	O_{AG}	114	-0.566	C_{OB}	60	0.367	N_I	14	-0.707
C_{OB}	26	0.324	O_{AG}	95	-0.590	C_{OB}	70	0.343	N_I	23	-0.708
C_{OB}	17	0.320	N_I	32	-0.676	C_S	75	0.309	O_S	80	-0.763
C_{OB}	8	0.319	N_I	14	-0.680	C_S	73	0.308	O_{OB}	58	-0.867
C_S	102	0.301	N_I	5	-0.681	C_S	77	0.136	O_{OB}	59	-0.888
C_S	71	0.301	N_I	23	-0.683	N_{AB}	40	-0.480			
C_S	77	0.299	O_S	82	-0.702						
C_{OB}	99	0.294	O_S	107	-0.702						
C_{OB}	66	0.294	O_S	88	-0.702						
C_{OB}	35	0.290	O_S	86	-0.723						
C_{OB}	74	0.289	O_S	92	-0.723						
C_S	79	0.281	O_S	111	-0.723						
C_S	69	0.280	O_S	84	-0.729						
C_S	104	0.280	O_S	109	-0.730						
C_S	81	0.199	O_S	90	-0.730						

NBO Charges ZnPc-1B						NBO Charges ZnPc-1C					
Atom		**Q**	**Atom**		**Q**	**Atom**		**Q**	**Atom**		**Q**
C_{AG}	94	0.825	C_S	107	0.197	C_{Pc}	28	0.439	C_S	101	0.196
C_{Pc}	19	0.444	N_{AB}	38	-0.496	C_{Pc}	10	0.439	C_S	79	0.195
C_{Pc}	22	0.441	N_{AB}	37	-0.498	C_{Pc}	1	0.438	N_{AB}	40	-0.500

C_{Pc}	10	0.441	N_{AB}	39	-0.500	C_{Pc}	19	0.438	N_{AB}	39	-0.500
C_{Pc}	4	0.440	N_{AB}	40	-0.502	C_{Pc}	13	0.437	N_{AB}	37	-0.500
C_{Pc}	1	0.439	O_{OB}	53	-0.509	C_{Pc}	31	0.437	N_{AB}	38	-0.501
C_{Pc}	13	0.435	O_{OB}	64	-0.514	C_{Pc}	22	0.436	O_{OB}	62	-0.514
C_{Pc}	28	0.432	O_{OB}	99	-0.514	C_{Pc}	4	0.436	O_{OB}	93	-0.514
C_{Pc}	31	0.431	O_{OB}	65	-0.514	C_{OB}	35	0.319	O_{OB}	63	-0.515
C_{OB}	54	0.338	O_{AG}	97	-0.613	C_{OB}	17	0.318	O_{OB}	53	-0.515
C_{OB}	17	0.321	N_I	32	-0.676	C_{OB}	8	0.318	N_I	5	-0.681
C_{OB}	26	0.320	N_I	14	-0.680	C_{OB}	26	0.315	N_I	23	-0.681
C_{OB}	8	0.319	N_I	5	-0.681	C_S	97	0.301	N_I	14	-0.681
C_S	103	0.301	N_I	23	-0.682	C_S	69	0.301	N_I	32	-0.681
C_S	71	0.301	O_S	82	-0.702	C_S	75	0.300	O_S	80	-0.702
C_S	77	0.300	O_S	108	-0.702	C_{OB}	72	0.296	O_S	86	-0.702
C_{OB}	100	0.294	O_S	88	-0.702	C_{OB}	94	0.296	O_S	102	-0.702
C_{OB}	66	0.294	O_{AG}	95	-0.717	C_{OB}	64	0.295	O_{AG}	108	-0.708
C_{OB}	74	0.292	O_S	92	-0.723	C_S	77	0.282	O_S	90	-0.723
C_{OB}	35	0.290	O_S	112	-0.723	C_S	99	0.280	O_S	106	-0.723
C_S	79	0.281	O_S	86	-0.723	C_S	67	0.280	O_S	84	-0.723
C_S	69	0.280	O_S	84	-0.730	C_{OB}	54	0.276	O_{AG}	111	-0.725
C_S	105	0.280	O_S	90	-0.730	C_{AG}	59	0.269	O_S	88	-0.730
C_S	81	0.198	O_S	110	-0.730	C_{AG}	61	0.269	O_S	104	-0.730
C_S	73	0.197				C_S	71	0.197	O_S	82	-0.730

NBO Charges SiPc-1B

Atom		Q	Atom		Q
C_{AG}	84	0.821	N_{AB}	38	-0.481
C_{Pc}	13	0.456	N_{AB}	37	-0.483
C_{Pc}	28	0.455	N_{AB}	39	-0.486
C_{Pc}	10	0.454	O_{AG}	85	-0.638
C_{Pc}	19	0.454	N_I	32	-0.703
C_{Pc}	31	0.453	N_I	5	-0.704
C_{Pc}	4	0.453	N_I	14	-0.705
C_{Pc}	1	0.452	O_S	78	-0.705
C_{Pc}	22	0.452	N_I	23	-0.705
C_{OB}	60	0.355	O_S	82	-0.705
C_{OB}	70	0.343	O_{AG}	86	-0.724
C_S	75	0.308	O_S	80	-0.764
C_S	73	0.308	O_{OB}	58	-0.874
C_S	77	0.136	O_{OB}	59	-0.887
N_{AB}	40	-0.481			

NBO Charges SiPc-1C

Atom		Q	Atom		Q
C_{Pc}	28	0.455	N_{AB}	40	-0.482
C_{Pc}	13	0.455	N_{AB}	38	-0.482
C_{Pc}	4	0.454	N_{AB}	37	-0.486
C_{Pc}	19	0.453	N_{AB}	39	-0.486
C_{Pc}	1	0.453	N_I	23	-0.699
C_{Pc}	31	0.452	N_I	32	-0.700
C_{Pc}	10	0.452	N_I	14	-0.700
C_{Pc}	22	0.451	N_I	5	-0.701
C_{OB}	69	0.345	O_S	77	-0.705
C_{OB}	60	0.311	O_S	81	-0.706
C_S	74	0.307	O_{AG}	85	-0.709
C_S	72	0.307	O_{AG}	83	-0.735
C_{AG}	65	0.286	O_S	79	-0.764
C_{AG}	67	0.234	O_{OB}	59	-0.886
C_S	76	0.135	O_{OB}	58	-0.891

C_{AG}: Anchor group carbon, **C_{Pc}:** Phthalocyanine carbon, **C_{OB}:** Oxygen bridge carbon, **C_S:** Substituent carbon, **N_{AB}:** Aza bridge nitrogen, **O_{OB}:** Oxygen bridge, **O_{AG}:** Anchor group oxygen, **N_I:** Isoindolic nitrogen and **O_S:** Substituent oxygen.

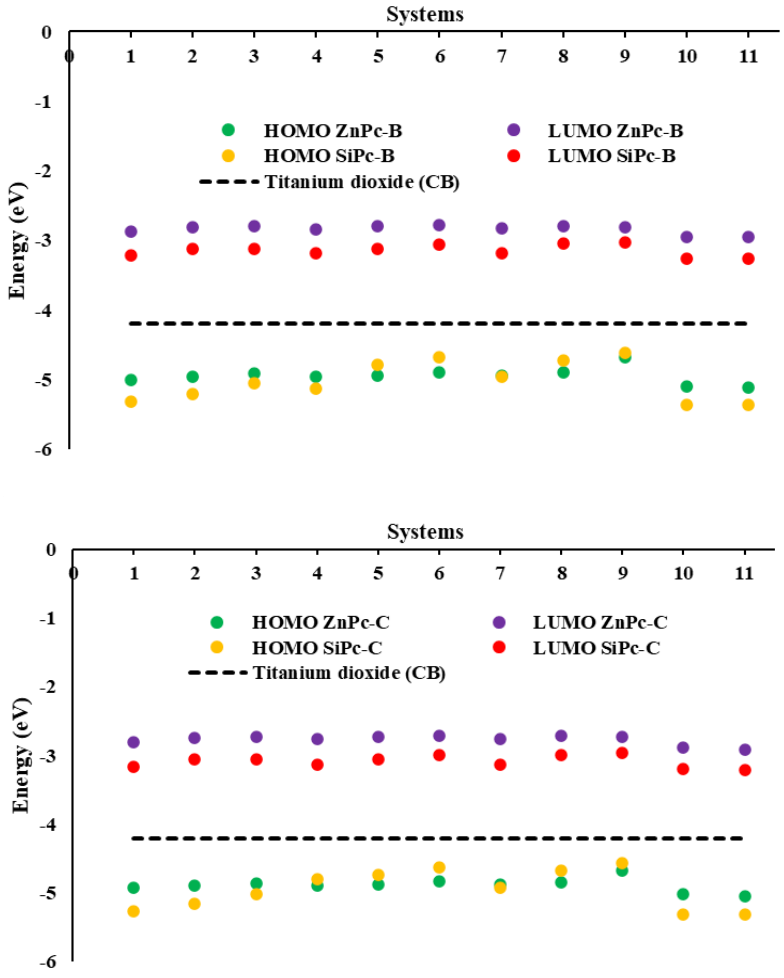

Figure S1. Energy values of the frontier molecular orbitals for ZnPc y SiPc with carboxyl **(B)** and catechol **(C)** anchoring groups.

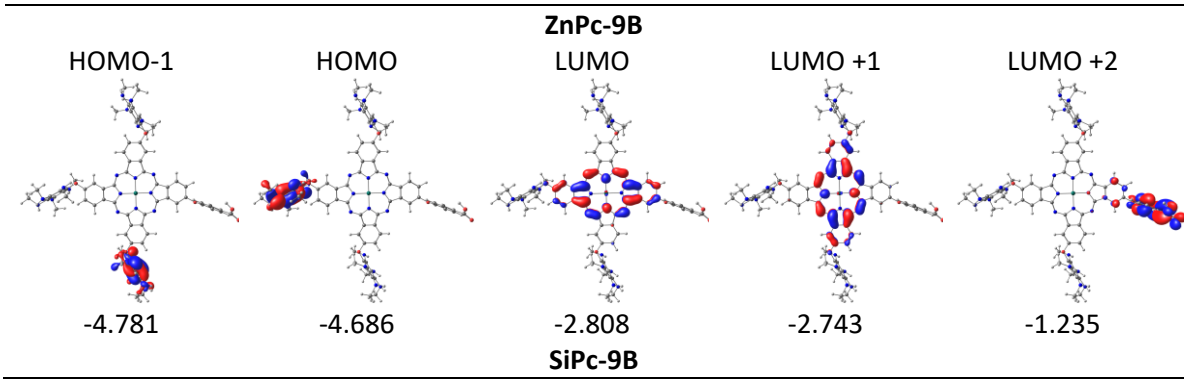

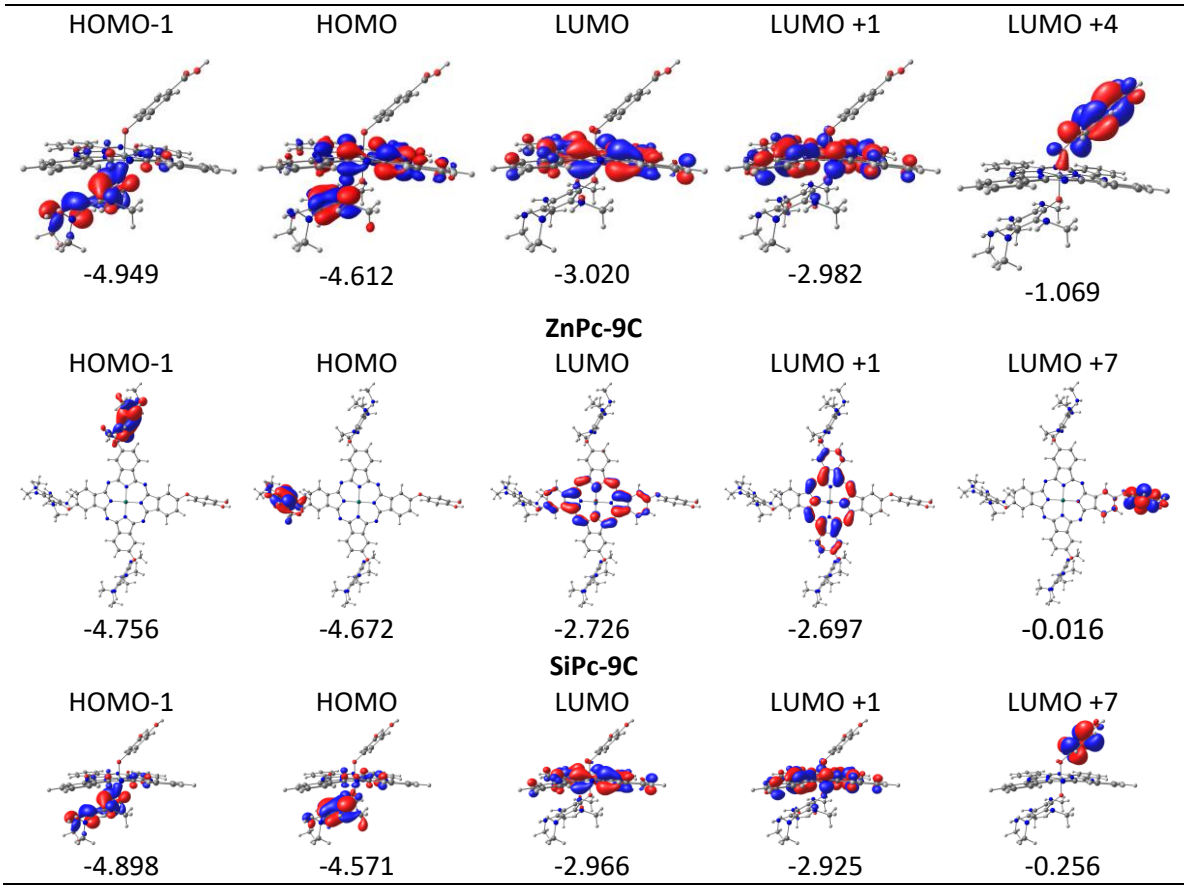

Figure S2. Surfaces of frontier molecular orbitals for **9B** (carboxyl anchor group) and **9C** (catechol anchor group) calculated in the solution phase.

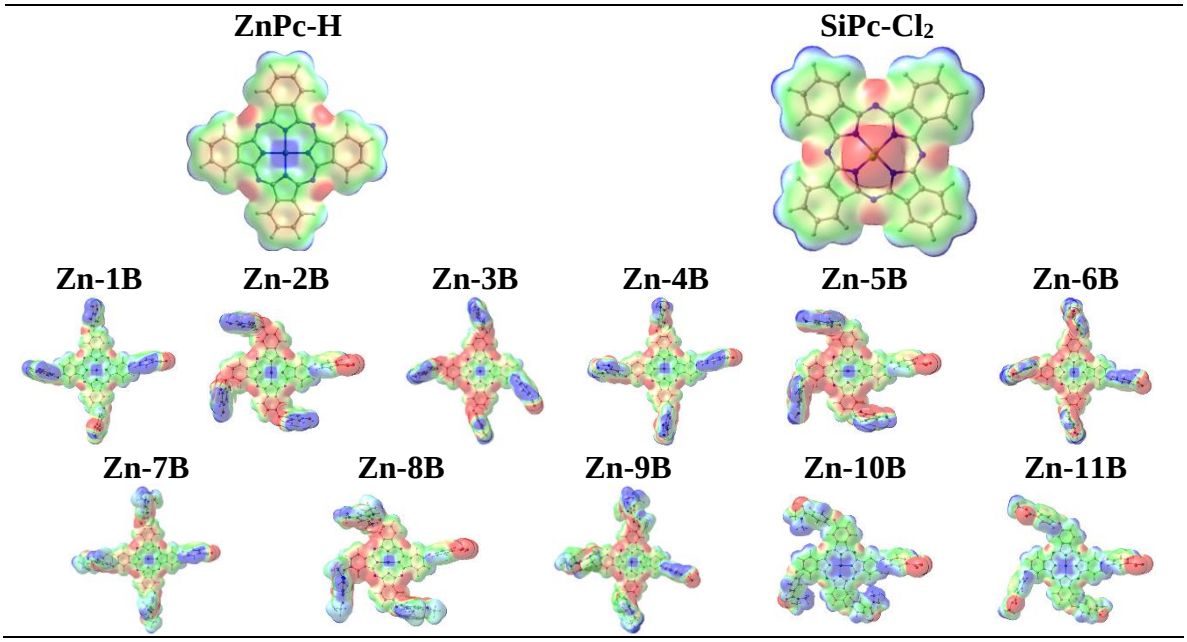

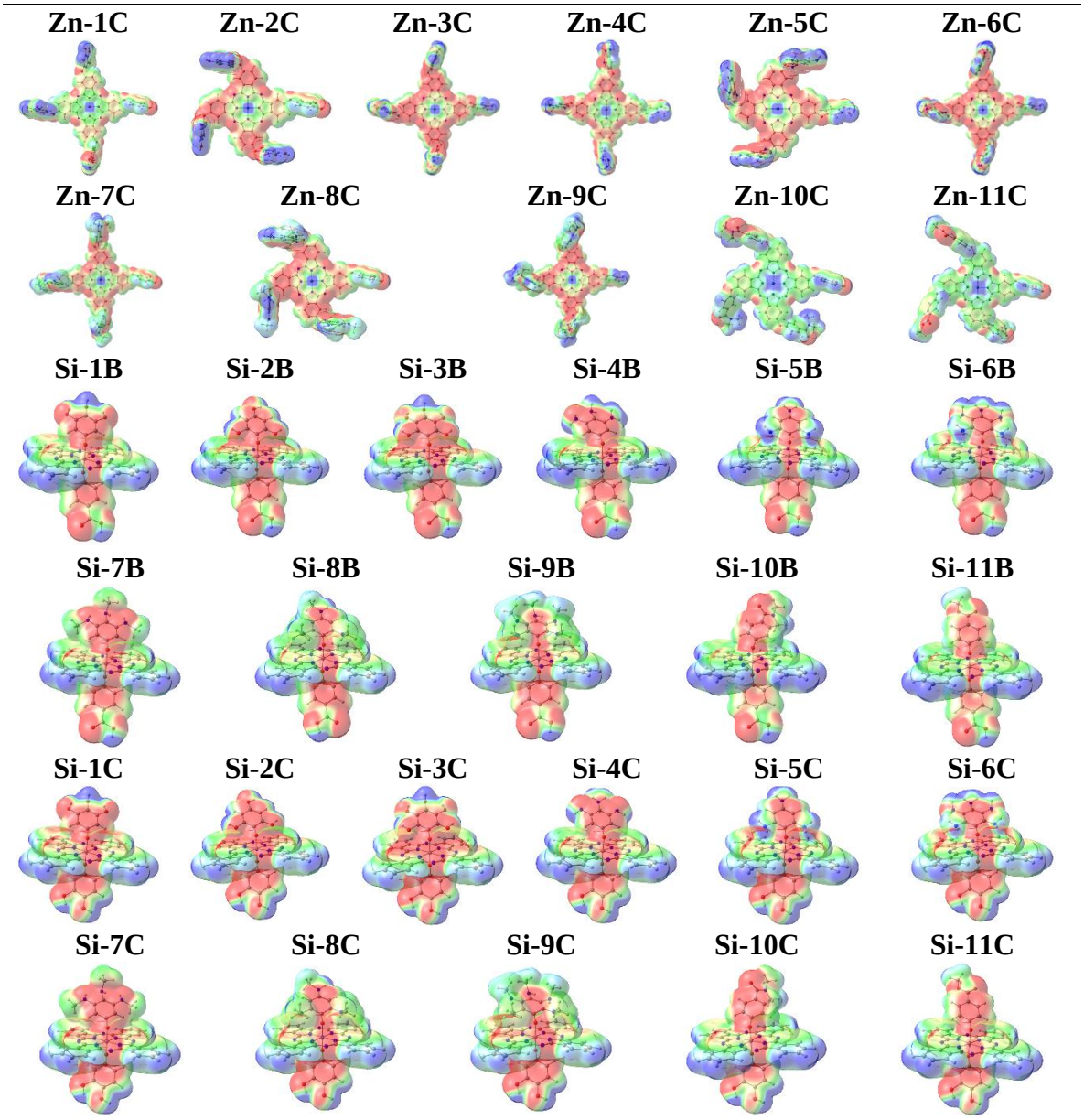

Figure S3. Surfaces of molecular electrostatic potential mapped into the charge density isosurface of 0.002 electrons/bohr^3 for MPcs with carboxyl (B) and catechol (C) anchoring group and without substituents.

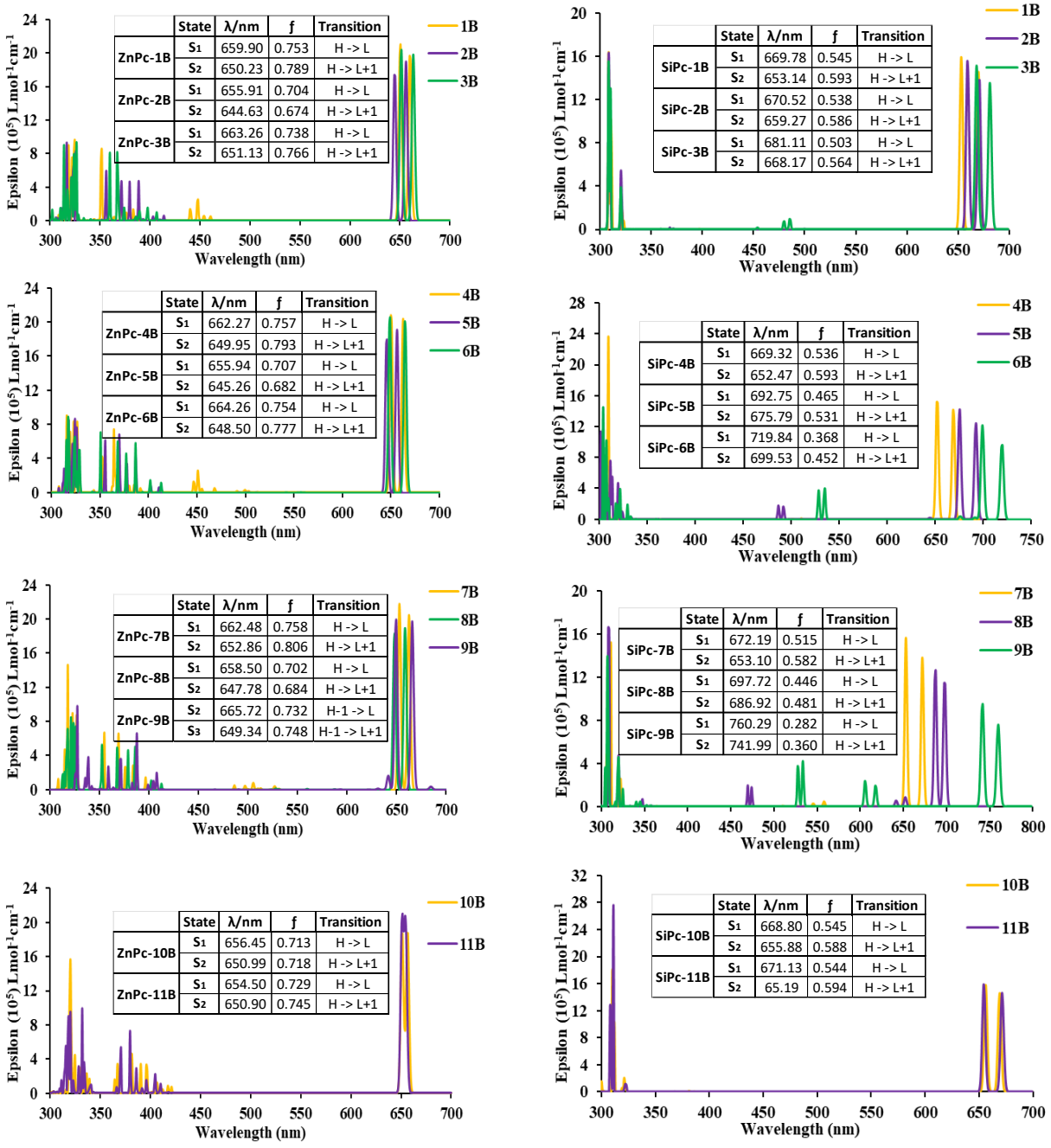

	State	λ/nm	ƒ	Transition
ZnPc-1B	S1	659.90	0.753	H -> L
	S2	650.23	0.789	H -> L+1
ZnPc-2B	S1	655.91	0.704	H -> L
	S2	644.63	0.674	H -> L+1
ZnPc-3B	S1	663.26	0.738	H -> L
	S2	651.13	0.766	H -> L+1

	State	λ/nm	ƒ	Transition
SiPc-1B	S1	669.78	0.545	H -> L
	S2	653.14	0.593	H -> L+1
SiPc-2B	S1	670.52	0.538	H -> L
	S2	659.27	0.586	H -> L+1
SiPc-3B	S1	681.11	0.503	H -> L
	S2	668.17	0.564	H -> L+1

	State	λ/nm	ƒ	Transition
ZnPc-4B	S1	662.27	0.757	H -> L
	S2	649.95	0.793	H -> L+1
ZnPc-5B	S1	655.94	0.707	H -> L
	S2	645.26	0.682	H -> L+1
ZnPc-6B	S1	664.26	0.754	H -> L
	S2	648.50	0.777	H -> L+1

	State	λ/nm	ƒ	Transition
SiPc-4B	S1	669.32	0.536	H -> L
	S2	652.47	0.593	H -> L+1
SiPc-5B	S1	692.75	0.465	H -> L
	S2	675.79	0.531	H -> L+1
SiPc-6B	S1	719.84	0.368	H -> L
	S2	699.53	0.452	H -> L+1

	State	λ/nm	ƒ	Transition
ZnPc-7B	S1	662.48	0.758	H -> L
	S2	652.86	0.806	H -> L+1
ZnPc-8B	S1	658.50	0.702	H -> L
	S2	647.78	0.684	H -> L+1
ZnPc-9B	S2	665.72	0.732	H-1 -> L
	S3	649.34	0.748	H-1 -> L+1

	State	λ/nm	ƒ	Transition
SiPc-7B	S1	672.19	0.515	H -> L
	S2	653.10	0.582	H -> L+1
SiPc-8B	S1	697.72	0.446	H -> L
	S2	686.92	0.481	H -> L+1
SiPc-9B	S1	760.29	0.282	H -> L
	S2	741.99	0.360	H -> L+1

	State	λ/nm	ƒ	Transition
ZnPc-10B	S1	656.45	0.713	H -> L
	S2	650.99	0.718	H -> L+1
ZnPc-11B	S1	654.50	0.729	H -> L
	S2	650.90	0.745	H -> L+1

	State	λ/nm	ƒ	Transition
SiPc-10B	S1	668.80	0.545	H -> L
	S2	655.88	0.588	H -> L+1
SiPc-11B	S1	671.13	0.544	H -> L
	S2	65.19	0.594	H -> L+1

Figure S4. UV-Vis spectra calculated by TD-DFT with the **carboxyl anchor group** as the anchoring group. Left: ZnPc, Right: SiPc. The excitations corresponding to the Q-band region are included in the center of the figure.

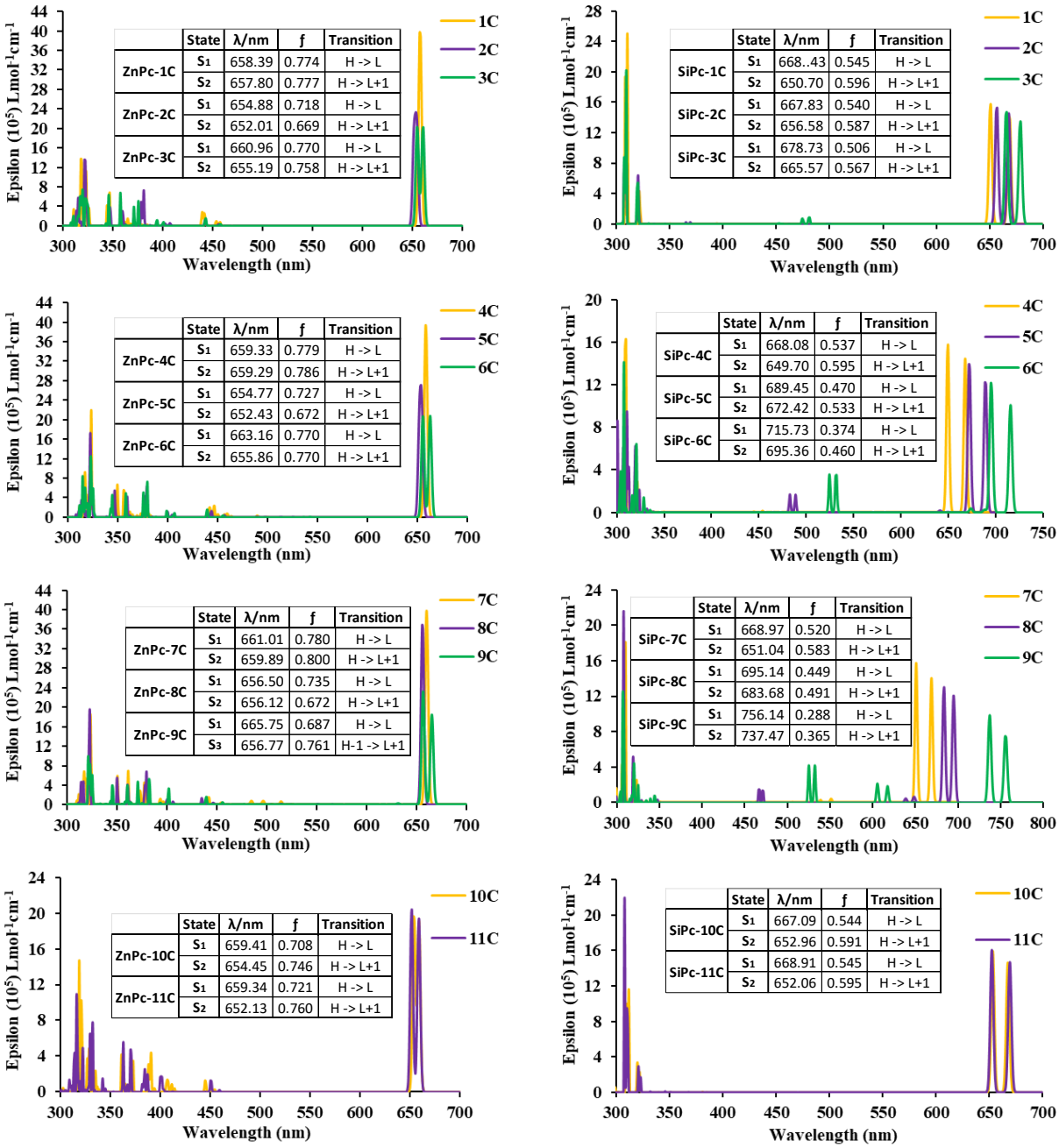

	State	λ/nm	ƒ	Transition
ZnPc-1C	S_1	658.39	0.774	H -> L
	S_2	657.80	0.777	H -> L+1
ZnPc-2C	S_1	654.88	0.718	H -> L
	S_2	652.01	0.669	H -> L+1
ZnPc-3C	S_1	660.96	0.770	H -> L
	S_2	655.19	0.758	H -> L+1

	State	λ/nm	ƒ	Transition
SiPc-1C	S_1	668..43	0.545	H -> L
	S_2	650.70	0.596	H -> L+1
SiPc-2C	S_1	667.83	0.540	H -> L
	S_2	656.58	0.587	H -> L+1
SiPc-3C	S_1	678.73	0.506	H -> L
	S_2	665.57	0.567	H -> L+1

	State	λ/nm	ƒ	Transition
ZnPc-4C	S_1	659.33	0.779	H -> L
	S_2	659.29	0.786	H -> L+1
ZnPc-5C	S_1	654.77	0.727	H -> L
	S_2	652.43	0.672	H -> L+1
ZnPc-6C	S_1	663.16	0.770	H -> L
	S_2	655.86	0.770	H -> L+1

	State	λ/nm	ƒ	Transition
SiPc-4C	S_1	668.08	0.537	H -> L
	S_2	649.70	0.595	H -> L+1
SiPc-5C	S_1	689.45	0.470	H -> L
	S_2	672.42	0.533	H -> L+1
SiPc-6C	S_1	715.73	0.374	H -> L
	S_2	695.36	0.460	H -> L+1

	State	λ/nm	ƒ	Transition
ZnPc-7C	S_1	661.01	0.780	H -> L
	S_2	659.89	0.800	H -> L+1
ZnPc-8C	S_1	656.50	0.735	H -> L
	S_2	656.12	0.672	H -> L+1
ZnPc-9C	S_1	665.75	0.687	H -> L
	S_3	656.77	0.761	H-1 -> L+1

	State	λ/nm	ƒ	Transition
SiPc-7C	S_1	668.97	0.520	H -> L
	S_2	651.04	0.583	H -> L+1
SiPc-8C	S_1	695.14	0.449	H -> L
	S_2	683.68	0.491	H -> L+1
SiPc-9C	S_1	756.14	0.288	H -> L
	S_2	737.47	0.365	H -> L+1

	State	λ/nm	ƒ	Transition
ZnPc-10C	S_1	659.41	0.708	H -> L
	S_2	654.45	0.746	H -> L+1
ZnPc-11C	S_1	659.34	0.721	H -> L
	S_2	652.13	0.760	H -> L+1

	State	λ/nm	ƒ	Transition
SiPc-10C	S_1	667.09	0.544	H -> L
	S_2	652.96	0.591	H -> L+1
SiPc-11C	S_1	668.91	0.545	H -> L
	S_2	652.06	0.595	H -> L+1

Figure S5. UV-Vis spectra calculated by TD-DFT with the **catechol anchor group** as the anchoring group. Left: ZnPc, Right: SiPc. The excitations corresponding to the Q-band region are included in the center of the figure.

Table S1. Adsorption (E_{ads}) and interaction (E_{int}) energies calculated at the molecular level at the GGA-PBE/Double ζ basis set/PseudDojo theory level.

ZnPc	**1A**	**2A**	**3A**	**4A**	**5A**	**6A**	**7A**	**8A**	**9A**	**10A**	**11A**
E_{ads}	-1.211	-0.946	-0.993	-1.111	-1.252	-1.335	-1.314	-1.307	-1.588	-1.320	-1.036
E_{int}	-1.482	-1.367	-1.440	-1.447	-1.524	-1.729	-1.595	-1.639	-1.891	-1.616	-1.339
ZnPc	**1B**	**2B**	**3B**	**4B**	**5B**	**6B**	**7B**	**8B**	**9B**	**10B**	**11B**
E_{ads}	-0.827	-0.648	-0.696	-0.646	-0.678	-1.566	-0.880	-1.139	-1.100	-0.610	-2.851
E_{int}	-4.522	-3.940	-3.890	-3.813	-3.813	-3.992	-4.381	-3.891	-3.994	-3.973	-3.979
SiPc	**1A**	**2A**	**3A**	**4A**	**5A**	**6A**	**7A**	**8A**	**9A**	**10A**	**11A**
E_{ads}	-1.639	-1.900	-1.721	-1.788	-2.063	-2.065	-1.627	-1.760	-1.531	-1.790	-1.538
E_{int}	-2.102	-2.264	-2.128	-2.078	-2.444	-2.502	-2.065	-2.161	-1.907	-2.206	-2.046
SiPc	**1B**	**2B**	**3B**	**4B**	**5B**	**6B**	**7B**	**8B**	**9B**	**10B**	**11B**
E_{ads}	-0.988	-1.036	-1.052	-1.039	-1.156	-1.320	-1.135	-1.185	-1.051	-0.989	-1.095
E_{int}	-4.911	-4.681	-4.633	-4.518	-4.836	-4.555	-4.576	-4.641	-4.590	-4.765	-4.610

Table S2. Comparison of some properties for systems adsorbed on different TiO_2 surfaces.

1 layer	**2 layers**	**3 layers**
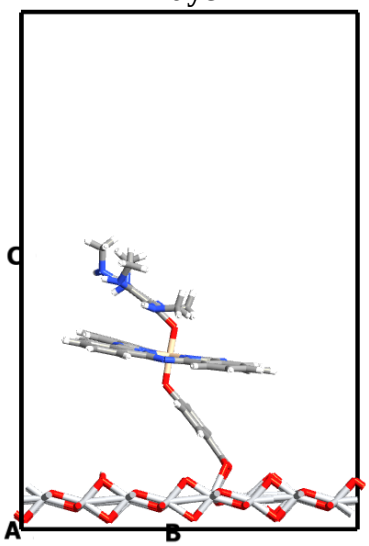	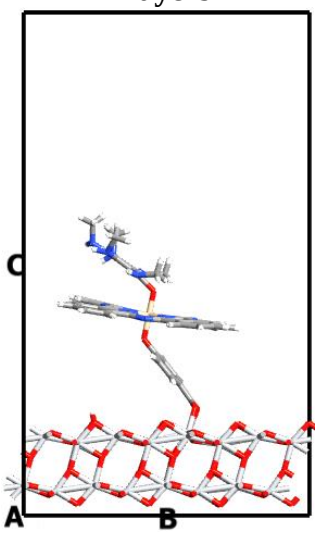	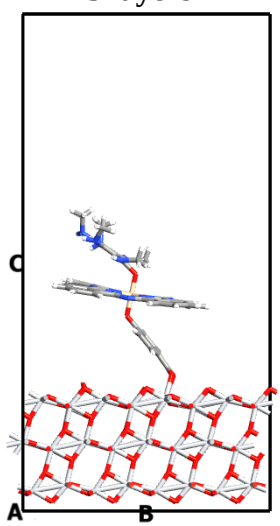
E_{int}= -4.911 eV BandGap=3.250 eV Valence band = -1.695 eV Conduction band = 1.555	E_{int}= -4.925 eV BandGap= 3.232 eV Valence band = -1.634 eV Conduction band = 1.598 eV	E_{int}= -5.009 eV BandGap= 3.324 eV Valence band = -1.688eV Conduction band = 1.636 eV
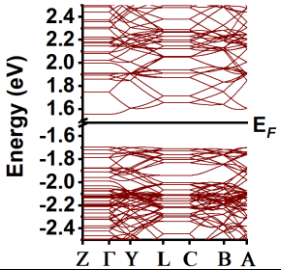	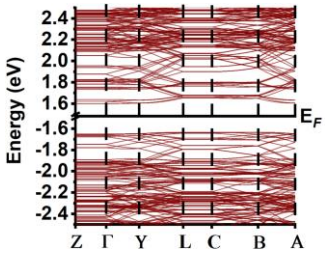	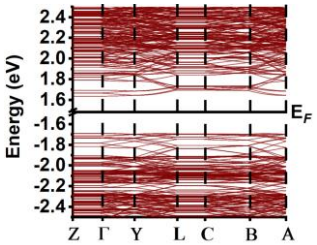

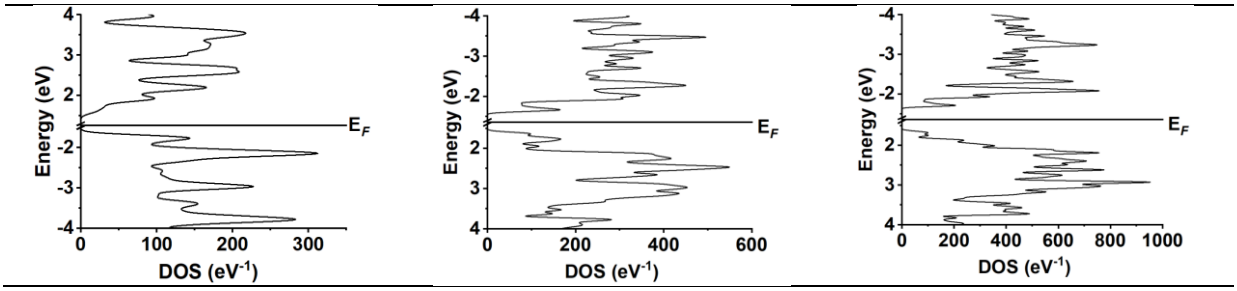

The calculation involved testing systems with one, two, and three semiconductor layers (TiO_2), comprising 253, 397, and 541 atoms, respectively. As seen in Table S2, interaction energies exhibited minimal changes, with the largest variation being 0.098 eV, observed between the single-layer and three-layer systems. Similarly, the energy band gap displayed no significant fluctuations, with the highest value recorded for the three-layer system at 3.324 eV and the lowest for the two-layer system at 3.232 eV. However, this difference remained below 0.1 eV, indicating marginal variation.

In the evaluation of band structure and density of states (DOS) for each surface, the analysis revealed that valence and conduction bands experienced negligible variations across different systems. The valence band ranged from -1.695 to -1.634 eV, while the conduction band ranged from 1.555 to 1.636 eV. In both cases, the variations were less than 0.1 eV, demonstrating convergence in these values concerning system size.

The main distinction lies in the number of bands in the band structure, resulting in a higher density of states as the system size increases. This increase stemmed from the greater number of atoms in the systems, leading to a higher count of electrons. Nevertheless, despite this, the band structure and DOS trend remained similar across the evaluated systems.

Consequently, the decision was made to focus on studying and analyzing adsorbed systems on the surface of one single layer. This choice was motivated by the lower number of atoms

in these systems, resulting in calculations that are more computationally efficient in terms of time and resources.

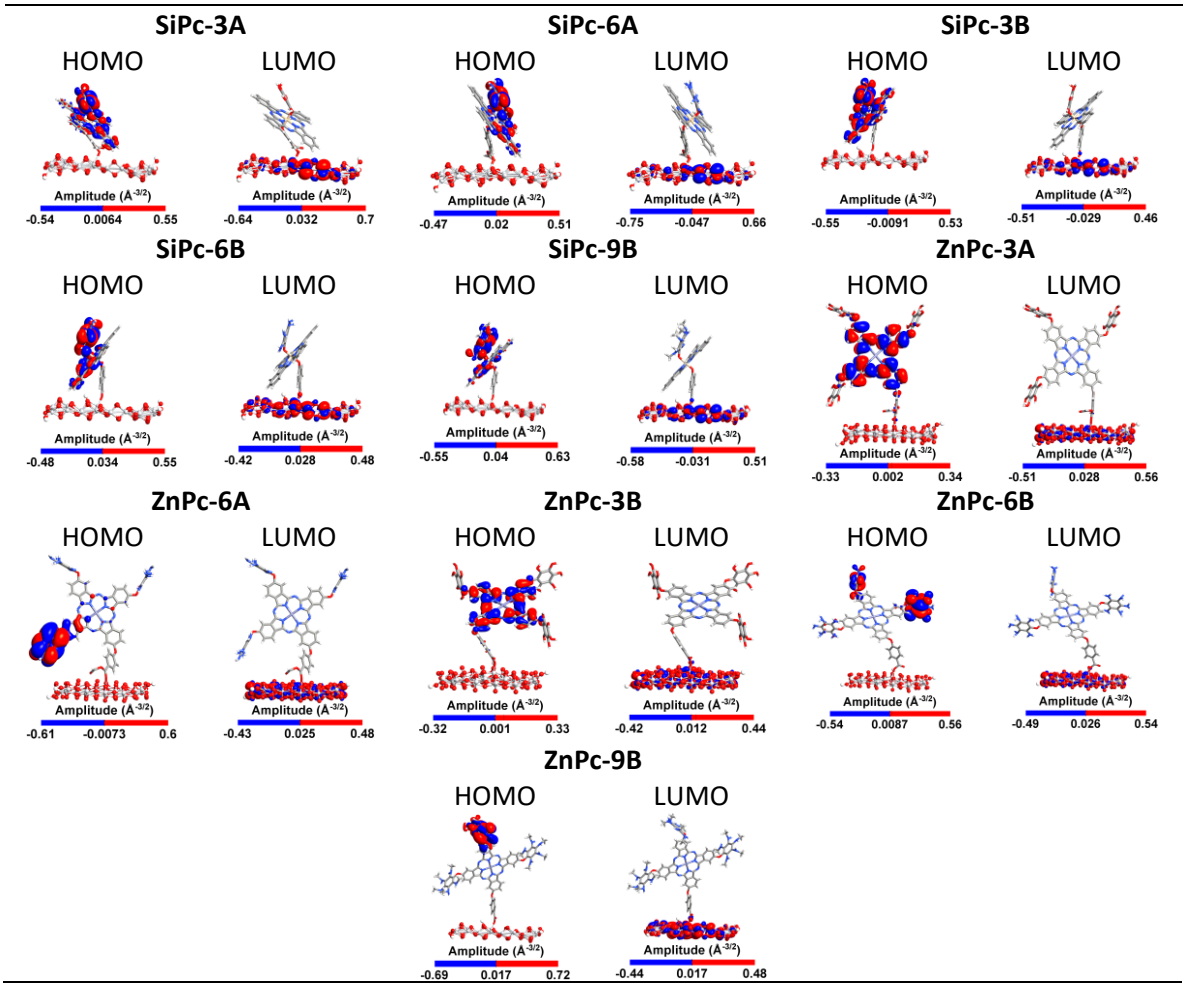

Figure S6. Surfaces of the frontier molecular orbitals calculated for the interaction dye-TiO_2.